Indium tin oxide-free and metal-free semitransparent organic solar cells

Yinhua Zhou, Hyeunseok Cheun, Seungkeun Choi, William J. Potscavage, Canek Fuentes-Hernandez et al.

Citation: Appl. Phys. Lett. **97**, 153304 (2010); doi: 10.1063/1.3499299
View online: http://dx.doi.org/10.1063/1.3499299
View Table of Contents: http://apl.aip.org/resource/1/APPLAB/v97/i15
Published by the American Institute of Physics.

Indium tin oxide-free and metal-free semitransparent organic solar cells

Yinhua Zhou, Hyeunseok Cheun, Seungkeun Choi, William J. Potscavage, Jr., Canek Fuentes-Hernandez, and Bernard Kippelen[a)]
Center for Organic Photonics and Electronics (COPE), School of Electrical and Computer Engineering, Georgia Institute of Technology, Atlanta, Georgia 30332, USA

(Received 12 August 2010; accepted 13 September 2010; published online 12 October 2010)

We report on indium tin oxide (ITO)-free and metal-free semitransparent organic solar cells with a high-conductivity poly(3,4-ethylenedioxythiophene):poly(styrenesulfonate) (PEDOT:PSS) (PH1000) as both the bottom and the top electrodes. The PH1000 film showed a conductivity of 680 ± 50 S/cm. A ZnO layer was used as an interlayer to produce an electron-selective electrode. The semitransparent devices with a structure of glass/PH1000/ZnO/poly(3-hexylthiophene):phenyl-C_{61}-butyric acid methyl ester/PEDOT:PSS (CPP 105 D)/PH1000 exhibited an average power conversion efficiency of 1.8% estimated for 100 mW/cm^2 air mass 1.5 global illumination. This geometry alleviates the need of vacuum deposition of a top electrode. © *2010 American Institute of Physics*. [doi:10.1063/1.3499299]

Organic solar cells have been attracting considerable attention due to their potential for low-cost, flexible, and large-area applications.[1–3] Power conversion efficiencies (PCEs) have reached 5%–7% with low-band gap materials.[4,5] Though their efficiencies are not as high as inorganic solar cells, organic solar cells can offer several inherent advantages. One very attractive feature of organic solar cells is the possibility to realize semitransparent solar cells which could be used to produce smart windows for buildings or cars that could generate power and be aesthetically pleasing at the same time. The see-through color can be adjusted by using organic active layers with tailored spectral transmission.

Until now, most semitransparent organic solar cells incorporated indium tin oxide (ITO) as both electrodes[6–9] or one of the electrodes.[10–12] However, the price of ITO is increasing due to its high demand in a wide variety of applications, which will increase the cost of ITO-based semitransparent devices accordingly. Furthermore, ITO is brittle, which limits device flexibility. To replace ITO in organic solar cells, high-conductivity poly(3,4-ethylenedioxythiophene):poly(styrenesulfonate) (PEDOT:PSS) has been used as the electrode in solar cells.[13] PEDOT:PSS is an intrinsically conductive polymer mixture, and its conductivity can vary over a wide range with the use of different additives.[14] PEDOT:PSS films can be prepared from aqueous solution and coated at low cost for large-area applications using spin-coating or printing.

Previously, high-conductivity PEDOT:PSS PH500 (H.C. Starck) as a replacement for ITO was proposed for the bottom electrode in solar cells.[15–17] The PCE values were 80%–90% of those in solar cells with an ITO electrode. Furthermore, the replacement of the top metal electrode with PEDOT:PSS PH500 has also been demonstrated by spin coating and spraying techniques.[18–21] To date, the only report of semitransparent solar cells using PEDOT:PSS as both the bottom and the top electrodes used a layer of ZnO nanoparticles on top of PEDOT:PSS as the electron-selective layer. However, these devices yielded poor rectification and PCE.[21]

In this paper, we report on semitransparent solar cells using high-conductivity PEDOT:PSS PH1000 (H.C. Starck) (hereafter referred to as PH1000) as both the bottom and the top electrodes. The device structure is shown in Fig. 1(a). A ZnO layer was deposited on the bottom PH1000 film by atomic layer deposition (ALD) to turn the electrode into an electron-selective electrode. A poly(3-hexylthiophene) (P3HT):phenyl-C_{61}-butyric acid methyl ester ($PC_{60}BM$) blend was used as the active layer. The top hole-selective electrode was comprised of a bilayer of PEDOT:PSS CPP 105 D (H.C. Starck) (hereafter referred to as CPP-PEDOT) and PH1000. The semitransparent devices with a structure of glass/PH1000/ZnO/P3HT:PC_{60}BM/CPP-PEDOT/PH1000 exhibited an average PCE of 1.8% es-

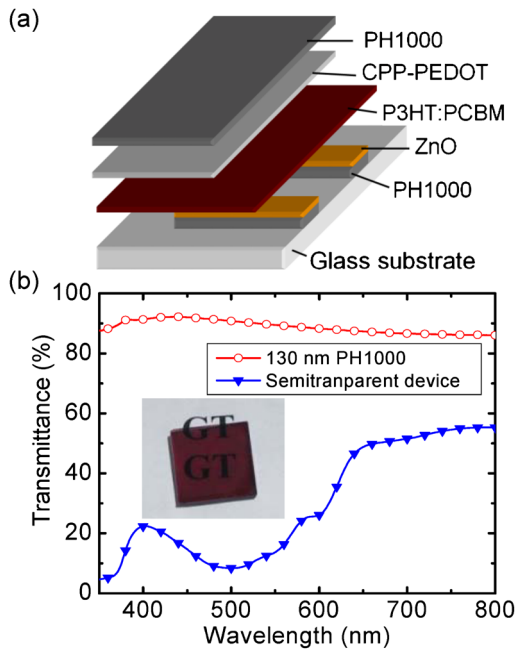

FIG. 1. (Color online) (a) Schematic structure of the semitransparent device with PH1000 as both the bottom and the top electrodes. (b) The transmittance of a 130-nm-thick PH1000 film on glass and a semitransparent device on glass. The inset shows a photograph of a device to illustrate its level of transparency.

[a)]Author to whom correspondence should be addressed. Electronic mail: kippelen@ece.gatech.edu.

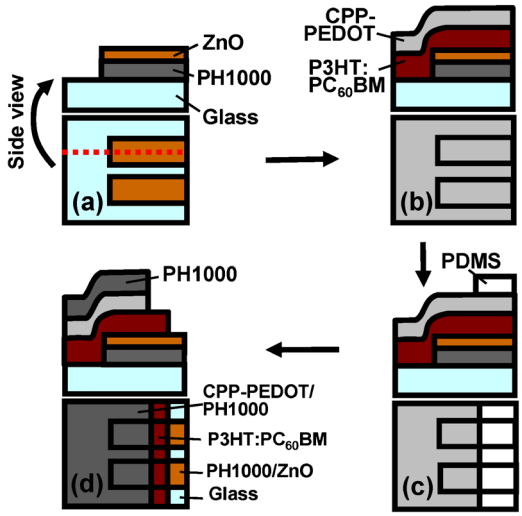

FIG. 2. (Color online) Fabrication process steps of the semitransparent devices with PH1000 as the bottom and the top electrodes. In each section of the figure, the bottom shows the top view and the top shows a cross-section through the dashed line.

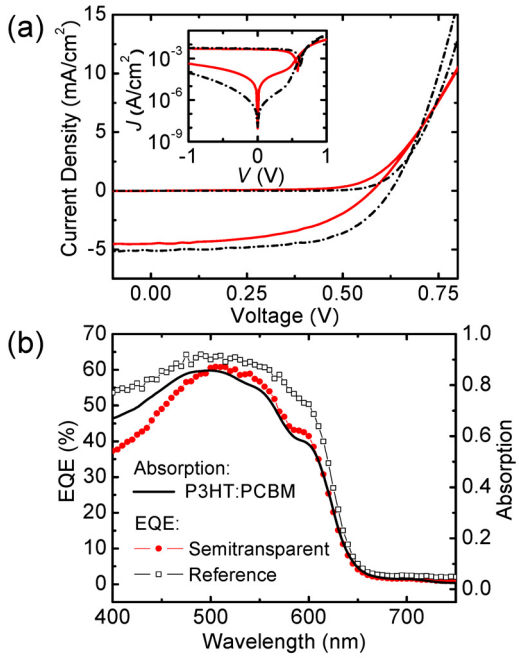

FIG. 3. (Color online) (a) *J-V* characteristics of a semitransparent device (solid line) and a reference device (dashed-dotted line) in the dark and under illumination. The inset is the *J-V* curves on semilog axes. (b) The EQE spectra of a semitransparent device and a reference device with the absorption spectrum of P3HT:PC_{60}BM (200 nm) on glass.

timated for 100 mW/cm^2 air mass 1.5 global (AM 1.5G) illumination. At the same time, the devices showed optical transmittance of 10 to 55% in the range from 400 to 800 nm [Fig. 1(b)].

To increase its conductivity, 5% dimethyl sulfoxide was added to the PH1000 solution. To evaluate the transmittance, work function, conductivity, and the role as the bottom electrode in semitransparent devices, 130-nm-thick PH1000 films were prepared by spin-coating on cleaned glass substrates at a speed of 1000 rpm for 40 s and annealing at 120 °C for 30 min in ambient air. Transmittance spectra of a PH1000 film on glass, a P3HT:PC_{60}BM film on glass and a semitransparent device were measured using a Varian Cary 5E spectrometer. Reflectance of a P3HT:PC_{60}BM film on glass was measured with a Shimadzu UV-3100 spectrometer. The conductivities of the PH1000 film and CPP-PEDOT film were measured using the transmission line method (TLM) with 200-nm-thick Cu electrodes thermally deposited on PH1000. Work function values were measured in air using a kelvin probe (Besocke Delta Phi) with a highly ordered pyrolytic graphite (HOPG) sample as the reference (work function of 4.5 eV). Contact angle values of PH1000 solution and CPP-PEDOT solution on P3HT:PC_{60}BM layers were measured using contact angle analyzer (SEO Phoenix 300).

The fabrication process steps of the semitransparent devices are shown in Fig. 2. A ZnO layer (40 nm) was deposited at 80 °C on a PH1000-coated glass substrate using a Savannah100 ALD system (Cambridge Nanotech Inc.). Then, PH1000/ZnO was patterned into two bottom electrodes by scraping with metal blades (BD Bard-Parker™) [Fig. 2(a)]. A solution of P3HT (4002-E, Rieke Metals):PC_{60}BM (Nano-C) was prepared by adding 2 ml of chlorobenzene to 40 mg of P3HT and 28 mg of PC_{60}BM. The active layer was spin coated at 700 rpm for 1 min and the substrate annealed at 160 °C for 10 min in a N_2 glove box. The thickness was 200 nm. A 90-nm-thick layer of CPP-PEDOT was spin-coated on the active layer at a speed of 5000 rpm for 60 s [Fig. 2(b)]. The CPP-PEDOT layer was patterned by adhering a polydimethylsiloxane (PDMS) layer to the unwanted area and peeling off the PDMS and CPP-PEDOT together. The samples were next annealed at 105 °C for 10 min in the glove box [Fig. 2(c)]. Finally, PH1000 (160 nm) was spin-coated on the patterned CPP-PEDOT area in ambient air. The PH1000 solution could only wet CPP-PEDOT but not the P3HT:PC_{60}BM layer. To provide electrical contact to the bottom PH1000/ZnO electrode, a strip of P3HT:PC_{60}BM was dissolved by using a tissue with chlorobenzene. Samples were annealed at 105 °C for 10 min in the glove box [Fig. 2(d)]. The effective area was around 10 mm^2. Before measurement, electrical contact to the PH1000 layers was made with silver paste. For comparison, devices with a conventional structure of ITO/PEDOT:PSS (4083)/P3HT:PC_{60}BM/Al were fabricated as reference devices. The P3HT:PC_{60}BM layer was identical to the one used in the semitransparent devices. Current density-voltage (*J-V*) characteristics were measured in the glove box using a source meter (Keithley 2400) controlled by a LABVIEW program. To test the solar cell properties under illumination, an Oriel lamp was used as the light source with an irradiance of 100 mW/cm^2. The spectral response of the photocurrent was measured in the glove box with a 175 W xenon lamp (ASB-XE-175EX, CVI) coupled to a monochromator.

The transmittance of PH1000 (130 nm) was 85%–90% in the visible-wavelength range as shown in Fig. 1(b). The sheet resistance of the 130-nm-thick PH1000 on glass substrates was measured to be 115 ± 10 Ω/sq. by the TLM method, which corresponded to a film conductivity of 680 ± 50 S/cm (averaged over four samples). The contact angle of PH1000 solution on a P3HT:PC_{60}BM layer was measured to be $93° \pm 2°$ averaged over three locations. The high contact angle makes it difficult to deposit a uniform PH1000 layer on top of the P3HT:PC_{60}BM layer by spin coating. In contrast, the CPP-PEDOT solution showed low contact angle of $31 \pm 2°$ on the P3HT:PC_{60}BM layer but a lower conductivity of 20 ± 2 S/cm. Therefore, a bilayer of PH1000 and CPP-PEDOT was used as the top electrode. The

measurement of the work function of PH1000 yielded a value of 5.02 ± 0.04 eV. After the deposition of a thin layer of ZnO on top, the work function of the bottom electron-selective electrode was 4.26 ± 0.04 eV (averaged over three locations).

Figure 3(a) shows the *J-V* characteristics of a semitransparent device and a reference device under illumination and in the dark. The semitransparent device shows good diode properties with a rectification ratio in the dark of around 10^2 at ± 1 V. The devices work better than the previously reported devices with ZnO nanoparticles, most likely due to the dense and uniform nature of the ZnO films grown by the ALD method.[22] Averaged over five devices, the semitransparent devices show an open-circuit voltage (V_{OC}) of 0.55 ± 0.03 V, a short-circuit current density (J_{SC}) of 4.4 ± 0.2 mA/cm^2, a fill factor (FF) of 0.45 ± 0.05, and a PCE of $1.1 \pm 0.2\%$ under the illumination of the Oriel lamp with an intensity of 100 mW/cm^2. To correct for spectral mismatch between the lamp and AM 1.5G, the expected values of $J_{SC\text{-}AM\ 1.5}$ under 100 mW/cm^2 AM 1.5G illumination were estimated by multiplying the external quantum efficiency (EQE) and AM 1.5G spectra and intergrating.[22] The $J_{SC\text{-}AM\ 1.5}$ was calculated to be 7.20 ± 0.03 mA/cm^2 and (PCE) under AM 1.5G is, therefore, estimated to be $1.8 \pm 0.3\%$. The reference devices show an average V_{OC} of 0.62 ± 0.01 V, J_{SC} of 8.50 ± 0.4 mA/cm^2, FF of 0.59 ± 0.01, and PCE of $3.1 \pm 0.2\%$ estimated for 100 mW/cm^2 AM 1.5G illumination. The values of J_{SC} of the semitransparent devices are around 85% of those of the reference devices, close to those in a previous report.[23] The lower J_{SC} is attributed to the lack of a highly reflective back electrode in the semitransparent devices. The lower FF of semitransparent solar cells is mainly attributed to the higher resistance of PH1000 electrodes compared with the combination of Al and ITO in reference solar cells. However, the effects of the larger sheet resistance of polymer electrodes compared with ITO and metal electrodes can be minimized by incorporating metal grid electrodes[24] or by making large area devices using a stripe geometry.

Figure 3(b) shows a comparison of the EQE spectra of a semitransparent device with that of a reference device. It can be seen that the EQE spectrum of the semitransparent device is narrower and reaches smaller values than that of the reference device. To compare the EQE spectra with the intrinsic absorption of the active layer, the absorption (A) spectrum of a P3HT:$PC_{60}BM$ film deposited on a glass substrate was calculated as $A = 1 - T - R$, by measuring its transmittance (T) and reflectance (R). The absorption spectrum of a P3HT:$PC_{60}BM$ film (200 nm) is also shown in Fig. 3(b). As expected from the semitransparent nature of the device, the shape of its EQE spectrum resembles that of the absorption spectrum of the P3HT:$PC_{60}BM$ film. In reference devices with the Al reflector, the EQE is increased because light can go multiple times through the device. This increase is more evident in places where the active layer does not absorb light strongly, on both sides of the absorption peak. This increased absorption increases the EQE and yields larger values of the J_{SC} in the reference devices.

In summary, we reported semitransparent organic solar cells that use high-conductivity PEDOT:PSS PH1000 as both the bottom and the top electrodes. PH1000 showed a conductivity of 680 ± 50 S/cm. These ITO-free semitransparent organic solar cells exhibited an average PCE of 1.8% estimated for 100 mW/cm^2 AM 1.5G illumination. The transparent conducting polymer PEDOT:PSS PH1000 is therefore a promising candidate for the realization of ITO-free semitransparent solar cells. Furthermore, devices with such a geometry do not require the deposition of a metal electrode using vacuum techniques. Hence, they look promising candidates for low-cost see-through power-generating windows applications.

This material is based upon work supported in part by the STC Program of the National Science Foundation under Agreement No. DMR-0120967, by the Office of Naval Research, by AFOSR (BIONIC Center Grant No. FA9550-09-1-0162), and AFOSR (Grant No. FA9550-09-1-0418), and in part through the Center for Interface Science: Solar Electric Materials, an Energy Frontier Research Center funded by the U.S. Department of Energy, Office of Science, Office of Basic Energy Sciences under Award No. DE-SC0001084.

[1] B. Kippelen and J. L. Bredas, Energy Environ. Sci. **2**, 251 (2009).
[2] G. Dennler, M. C. Scharber, and C. J. Brabec, Adv. Mater. (Weinheim, Ger.) **21**, 1323 (2009).
[3] M. Helgesen, R. Sondergaard, and F. C. Krebs, J. Mater. Chem. **20**, 36 (2010).
[4] S. H. Park, A. Roy, S. Beaupre, S. Cho, N. Coates, J. S. Moon, D. Moses, M. Leclerc, K. Lee, and A. J. Heeger, Nat. Photonics **3**, 297 (2009).
[5] C. Piliego, T. W. Holcombe, J. D. Douglas, C. H. Woo, P. M. Beaujuge, and J. M. J. Frechet, J. Am. Chem. Soc. **132**, 7595 (2010).
[6] R. F. Bailey-Salzman, B. P. Rand, and S. R. Forrest, Appl. Phys. Lett. **88**, 233502 (2006).
[7] H. Schmidt, H. Flugge, T. Winkler, T. Bulow, T. Riedl, and W. Kowalsky, Appl. Phys. Lett. **94**, 243302 (2009).
[8] J. S. Huang, G. Li, and Y. Yang, Adv. Mater. (Weinheim, Ger.) **20**, 415 (2008).
[9] F. C. Chen, J. L. Wu, K. H. Hsieh, W. C. Chen, and S. W. Lee, Org. Electron. **9**, 1132 (2008).
[10] F. Nickel, A. Puetz, M. Reinhard, H. Do, C. Kayser, A. Colsmann, and U. Lemmer, Org. Electron. **11**, 535 (2010).
[11] J. Y. Lee, S. T. Connor, Y. Cui, and P. Peumans, Nano Lett. **10**, 1276 (2010).
[12] R. Koeppe, D. Hoeglinger, P. A. Troshin, R. N. Lyubovskaya, V. F. Razumov, and N. S. Sariciftci, ChemSusChem **2**, 309 (2009).
[13] F. L. Zhang, M. Johansson, M. R. Andersson, J. C. Hummelen, and O. Inganas, Adv. Mater. (Weinheim, Ger.) **14**, 662 (2002).
[14] S. Kirchmeyer and K. Reuter, J. Mater. Chem. **15**, 2077 (2005).
[15] Y. H. Zhou, F. L. Zhang, K. Tvingstedt, S. Barrau, F. H. Li, W. J. Tian, and O. Inganas, Appl. Phys. Lett. **92**, 233308 (2008).
[16] S. I. Na, S. S. Kim, J. Jo, and D. Y. Kim, Adv. Mater. (Weinheim, Ger.) **20**, 4061 (2008).
[17] E. Ahlswede, W. Muhleisen, M. Wahi, J. Hanisch, and M. Powalla, Appl. Phys. Lett. **92**, 143307 (2008).
[18] Y. F. Lim, S. Lee, D. J. Herman, M. T. Lloyd, J. E. Anthony, and G. G. Malliaras, Appl. Phys. Lett. **93**, 193301 (2008).
[19] Y. H. Zhou, F. H. Li, S. Barrau, W. J. Tian, O. Inganas, and F. L. Zhang, Sol. Energy Mater. Sol. Cells **93**, 497 (2009).
[20] Q. F. Dong, Y. H. Zhou, J. N. Pei, Z. Y. Liu, Y. W. Li, S. Y. Yao, J. B. Zhang, and W. J. Tian, Org. Electron. **11**, 1327 (2010).
[21] S. K. Hau, H. L. Yip, J. Y. Zou, and A. K. Y. Jen, Org. Electron. **10**, 1401 (2009).
[22] Y. H. Zhou, H. Cheun, W. J. Potscavage, Jr., C. Fuentes-Hernandez, S. J. Kim, and B. Kippelen, J. Mater. Chem. **20**, 6189 (2010).
[23] T. Ameri, G. Dennler, C. Waldauf, H. Azimi, A. Seemann, K. Forberich, J. Hauch, M. Scharber, K. Hingerl, and C. J. Brabec, Adv. Funct. Mater. **20**, 1592 (2010).
[24] S. Choi, W. J. Potscavage, Jr., and B. Kippelen, J. Appl. Phys. **106**, 054507 (2009).